Organic field-effect transistors fabricated with *N*,*N*′-substituted dialkyl-1,3,8,10-tetramethylquinacridone compounds

Zong-Xiang Xu,[1] Hai-Feng Xiang,[1,2] V. A. L. Roy,[1,3] Stephen Sin-Yin Chui,[1] Yue Wang,[4]
P. T. Lai,[2] and Chi-Ming Che[1,a)]
[1]*Department of Chemistry and HKU-CAS Joint Laboratory on New Materials,
The University of Hong Kong, Pokfulam Road, Hong Kong, Hong Kong*
[2]*Department of Electrical and Electronic Engineering, The University of Hong Kong, Pokfulam Road,
Hong Kong, Hong Kong*
[3]*Department of Physics and Materials Science, City University of Hong Kong, Tat Chee Avenue,
Kowloon, Hong Kong*
[4]*Key Laboratory of Supramolecular Structure and Materials, College of Chemistry, Jilin University,
Changchun 130021, People's Republic of China*

(Received 8 April 2009; accepted 26 August 2009; published online 22 September 2009)

A series of robust and inexpensive *p*-type organic semiconductors 1,3,8,10-tetramethyl quinacridone compounds was prepared. These quinacridone compounds bearing *N*,*N*′-disubstituted long *N*-alkyl chains self-organize into highly oriented crystalline films, leading to high performance organic thin film transistors with the best field-effect mobility, on/off ratio, and threshold voltage being 1.6×10^{-1} cm^2 V^{-1} s^{-1}, 1×10^4, and -17 V, respectively. The effects of methyl substituent and *N*-alkyl chain length of the quinacridone compounds together with the molecular packing on the field-effect mobility are discussed. © *2009 American Institute of Physics*. [doi:10.1063/1.3233961]

Organic thin film transistors (OTFTs) have important applications in electronics including sensors,[1] light-emitting devices,[2] and memory devices.[3] Compared with silicon-based devices, the fabrication process of OTFT is simple and low cost and has a high compatibility with conventional soft lithography.[4] To develop inexpensive and robust organic semiconductor materials that possess high field-effect mobility, much attention has been focused on *p*-type pentacene and derivatives.[5,6] Nonetheless, multisteps are needed for the synthesis and modification of pentacene compounds. In the context of developing OTFT materials, π-conjugated organic compounds with a rigid and fused-ring structure are of particular interest.[7–9]

Quinacridone compounds are chemically stable and widely utilized as light-emitting[10–12] and photoconductive materials.[13] These materials are relatively inexpensive, soluble in common organic solvents, and could be readily modified. In this work, a series of *N*,*N*′-dialkyl quinacridone (QA) compounds—QA-C$_2$, QA-C$_4$, QA-C$_6$, and QA-C$_8$—and *N*,*N*′-dialkyl-1,3,8,10-tetramethylquinacridone (TMQA) compounds—TMQA-C$_4$, TMQA-C$_6$, TMQA-C$_8$, and TMQA-C$_{16}$ (Fig. 1)—were prepared according to the literature methods.[10,14] The charge transport properties of these compounds for OTFT applications have been investigated.

The QA and TMQA compounds were used to fabricate organic transistors using a bottom-contact substrate-gate structure by high-vacuum evaporation and measured using the same literature method.[15] The surface morphology and crystallinity of the thin films in the OTFT devices fabricated with these compounds were studied by scanning electron microscopy (SEM) and grazing incidence x-ray diffraction (GIXRD).

The thermal stability of the QA or TMQA compounds and performance of the as-fabricated devices are listed in the Table I. Most of the compounds examined have a decomposition temperature (T_d) in the range of 373–416 °C.[14] Interestingly all TMQA compounds exhibited *p*-type field-effect behavior but all QA compounds exhibited no field-effect behavior. TMQA-C$_4$ showed a hole mobility (μ) of 2.4×10^{-3} cm^2 V^{-1} s^{-1}. An increase in the *N*-alkyl chain length (from hexyl to octyl chains) led to an increase in mobility (μ) of 5.0×10^{-3} cm^2 V^{-1} s^{-1} for TMQA-C$_6$ and 3.0×10^{-2} cm^2 V^{-1} s^{-1} for TMQA-C$_8$. However, further increase in the *N*-alkyl chain length led to a decrease in the mobility value, as revealed in the case of TMQA-C$_{16}$ ($\mu=2.1\times10^{-4}$ cm^2 V^{-1} s^{-1}). As depicted in Table I, the thin films derived from QA-C$_2$, QA-C$_4$, QA-C$_6$, and QA-C$_8$ showed no field effect. Octadecyltrichlorosilane (OTS) was deposited onto the substrate prior to the OTFT device fabrication to reduce the hydrophilicity of the SiO$_2$ surface.[16,17] Figure 2 shows the output and transfer characteristics of TMQA-C$_8$-based device with OTS-treated SiO$_2$/Si substrate before and after 100 cycles measurement. Upon increasing the gate voltage V_g, the drain current I_{ds} increases, revealing a *p*-type field-effect transistor (FET) behavior. The fresh sample showed a mobility of 0.16 cm^2 V^{-1} s^{-1} and current on/off ratio of 10^4. After 100 cycles measurement, the shape of the successive transfer curve remained unchanged, revealing an unchanged threshold voltage V_t, and the output curve

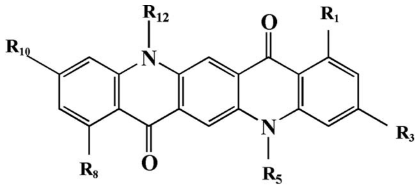

QA-C$_2$: R$_1$,R$_3$,R$_8$,R$_{10}$ = H; R$_5$, R$_{12}$ = C$_2$H$_5$ TMQA-C$_4$: R$_1$,R$_3$,R$_8$,R$_{10}$ = CH$_3$; R$_5$, R$_{12}$ = C$_4$H$_9$
QA-C$_4$: R$_1$,R$_3$,R$_8$,R$_{10}$ = H; R$_5$, R$_{12}$ = C$_4$H$_9$ TMQA-C$_6$: R$_1$,R$_3$,R$_8$,R$_{10}$ = CH$_3$; R$_5$, R$_{12}$ = C$_6$H$_{13}$
QA-C$_6$: R$_1$,R$_3$,R$_8$,R$_{10}$ = H; R$_5$, R$_{12}$ = C$_6$H$_{13}$ TMQA-C$_8$: R$_1$,R$_3$,R$_8$,R$_{10}$ = CH$_3$; R$_5$, R$_{12}$ = C$_8$H$_{17}$
QA-C$_8$: R$_1$,R$_3$,R$_8$,R$_{10}$ = H; R$_5$, R$_{12}$ = C$_8$H$_{17}$ TMQA-C$_{16}$: R$_1$,R$_3$,R$_8$,R$_{10}$ = CH$_3$; R$_5$, R$_{12}$ = C$_{16}$H$_{33}$

FIG. 1. Chemical structures of QA and TMQA compounds.

[a)] Electronic addresses: cmche@hku.hk and cmche@hkucc.hku.hk.

TABLE I. Thermal stability and field-effect characteristics of TMQA compounds.

Compound	T_d (°C)	μ ($cm^2 V^{-1} s^{-1}$)	I_{on}/I_{off}	Threshold voltage (V)
TMQA-C_4	375	2.4×10^{-3}	1×10^3	−4
TMQA-C_6	376	5.0×10^{-3}	1×10^2	−12
TMQA-C_8	388	3.0×10^{-2}	1×10^4	−20
TMQA-C_8 (OTS-treated)	⋯	1.6×10^{-1}	1×10^4	−17
TMQA-C_{16}	416	2.1×10^{-4}	1×10^2	−27.5
QA-C_2	375	⋯	⋯	⋯
QA-C_4	406	⋯	⋯	⋯
QA-C_6	393	⋯	⋯	⋯
QA-C_8	373	⋯	⋯	⋯

showed a decrease in the saturated current by less than 10% and a mobility of 0.15 $cm^2 V^{-1} s^{-1}$ corresponding to less than 10% decrease when compared with the initial mobility value. In addition, the devices could be operated under open atmosphere at room temperature and there was no change in the device performance. We did transient measurements on a TMQA-C_8-based FET device where a constant voltage was applied to the gate and drain (−40 V), while the current was measured as a function of time on the TMQA-C_8-based FET for more than 100 cycles. No decrease in the channel current was observed.[14] This device was kept in a glovebox. After a period of 2 years, this device showed a mobility of 0.14 $cm^2 V^{-1} s^{-1}$ corresponding to ~10% decrease in the initial mobility value, revealing the device stability.

Both crystallinity and morphology play important roles in the FET performance. FET behavior is usually observed for those materials that exhibit a regular crystalline packing arrangement. To acquire structural information, GIXRD patterns of thin films (100 nm thick) of QA and TMQA compounds deposited on SiO_2/Si substrate were recorded. In general, the QA-C_2 and QA-C_4 compounds formed thin films that displayed broad (full width at half maximum of ~0.8°–1.0° 2θ) and weak diffraction peaks (<100 counts/s), revealing the poor crystallinity and almost amorphous film structure [Fig. 3(a)]. The GIXRD pattern of the QA-C_8 thin film revealed two molecular orientations (2θ=6.36° and 2θ=7.75°) [Fig. 3(a)], both of which caused insulating effect with no FET behavior eventually observed. Although the film of QA-C_6 exhibited a single sharp diffraction peak, the lack of FET behavior could be attributed to film morphology in which case crystalline grains were found to be loosely packed as discussed in the latter section. In contrast, all TMQA thin films exhibited a strong single diffraction peak, revealing that the films were highly crystalline and textured with well-ordered molecular alignment in one favorable direction. The GIXRD pattern of the TMQA-C_4 thin film displayed a diffraction peak at 7.01°(2θ) corresponding to an interplanar *d*-space of 12.6 Å, which is close to the molecular size (approximately 13.0 Å derived from the single crystal x-ray data).[10] The *d*-space values of TMQA-C_6 (13.7 Å), TMQA-C_8 (17.0 Å), and TMQA-C_{16} (22.0 Å) thin films reflect that the *d*-space value increases with increasing *N*-alkyl chain length. All these *d*-space values are consistently shorter than the molecular size of the corresponding compounds (17.9 Å for TMQA-C_6, 22.9 Å for TMQA-C_8, and 42.9 Å for TMQA-C_{16}), which were estimated from the assumption that the *N*-alkyl chains have effective length of 1.2 Å per CH_2 unit and adopted *all-trans* configuration, similar to that found in the x-ray crystal structure of TMQA-C_4.[10] All TMQA compounds, except TMQA-C_4, have their molecular sizes larger than the observed *d*-space values, attributed to mutual interdigitation of the *N*-butyl chains throughout the neighboring molecular stacks.[14,18]

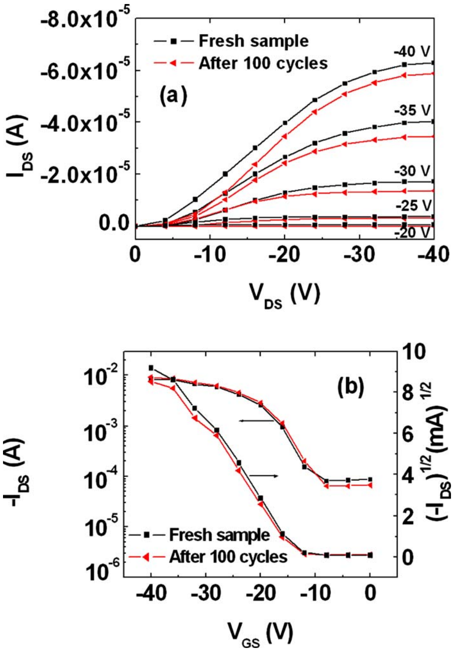

FIG. 2. (Color online) The current-voltage characteristics. (a) Output and (b) transfer characteristics of bottom-contact OTFT fabricated with TMQA-C_8 before and after 100 cycles measurement (with OTS treatment, channel length of 40 μm, and width of 3000 μm).

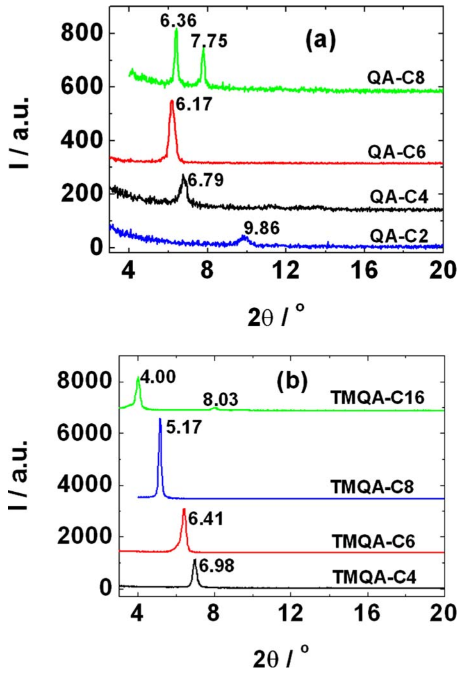

FIG. 3. (Color online) GIXRD patterns of vacuum-deposited thin films of (a) QA compounds and (b) TMQA compounds (the peak positions are shown in a 2θ scale).

The surface morphology of these thin films was revealed by their SEM images. As depicted in Fig. 4, the QA-C_4 [Fig. 4(b)] and QA-C_6 [Fig. 4(c)] thin films revealed discontinuous flat grains with considerable grain defects; consequently, the loosely packed crystalline grains led to no device performance. The as-deposited QA-C_2 film was almost covered by

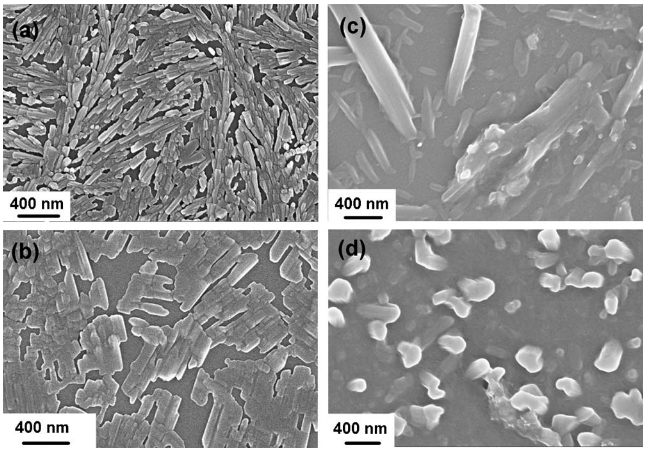

FIG. 4. SEM images of thin film samples made from (a) QA-C_2, (b) QA-C_4, (c) QA-C_6, and (d) QA-C_8 compounds deposited on the SiO_2/Si substrate.

platelike grains [Fig. 4(a)] and the QA-C_8 film was covered by continuous crystalline grains [Fig. 4(d)], whereas the thin films of TMQA compounds revealed continuous tightly packed crystals (Fig. 5) and this is favorable for charge transport. Upon increasing the N,N'-dialkyl chain length from N-butyl in TMQA-C_4 to N-octyl in TMQA-C_8, TMQA-C_8 thin film was found to have a densely packed crystal grain texture with little defect content.

The thin films of all QA compounds were poorly crystalline [Fig. 3(a)], consistent with the lack of field-effect mobility, whereas thin films of all TMQA compounds have a good field-effect mobility. This should be attributed to the effect of the peripheral 1,3,8,10-tetramethyl groups at the quinacridone core. The four C–H(methyl)···O=C interactions ($d=2.36$ Å) in the case of TMQA-C_4 substantially stabilize arrangement of molecules in the solid phase whereas the aryl hydrogen atoms of QA-C_4 merely lead to weak intermolecular interactions (2.54 Å).[10] Our previous study also showed that replace an ethyl group by a methyl group can significantly affect the field-effect mobility.[15] Compared with platinum(II) 2,3,7,8,12,13,17,18-octaethyl-21H,23H-porphyrin, the unsymmetrical peripheral substituents of platinum(II) etioporphyrin-I enables the molecules to efficiently pack with extensive lateral aggregations and $\pi\cdots\pi$ stacking interactions consequently leading to a high mobility of 0.32 $cm^2\,V^{-1}\,s^{-1}$.[15] Among all QA and TMQA compounds, the TMQA-C_8 thin film showed the strongest diffraction peak at 5.17° (2θ) (Fig. 3), revealing that this film had the highest degree of crystallinity. The unique spatial orientation of TMQA-C_8 molecules might reinforce the lateral molecular stacking parallel to the surface of the substrate, facilitating the in-plane charge transport of the film.[18] Therefore, the TMQA-C_8 thin film with a good morphology (Fig. 5) has the best field-effect mobility. But further increase in the N-alkyl chain as in the case of TMQA-C_{16} leads to a decrease in the field-effect mobility. The long N-alkyl chain of TMQA-C_{16} decreases the molecular packing, leading to a low crystallinity [Fig. 3(b)] and a low field-effect mobility.

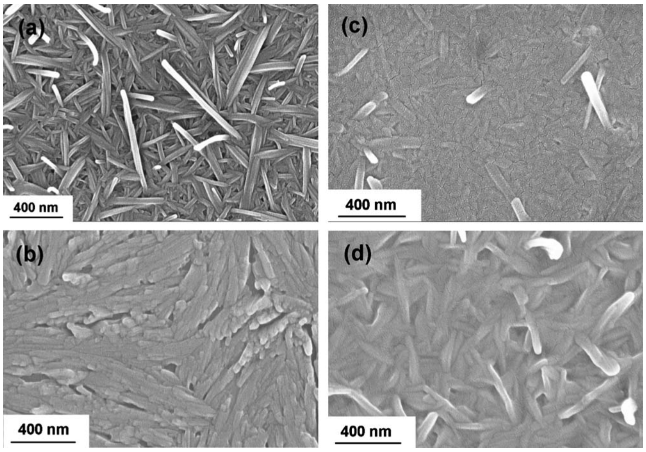

FIG. 5. SEM images of film samples made from (a) TMQA-C_4, (b) TMQA-C_6, (c) TMQA-C_8, and (d) TMQA-C_{16} compounds deposited on the SiO_2/Si substrate.

In summary, a series of QA and TMQA was synthesized to fabricate OTFTs by vacuum deposition method. The charge transport properties are strongly affected by the surface morphology, crystallinity, and molecular packing of the thin film. The crystal packing and field-effect mobility of thin films of TMQA compounds are affected by the length of N-alkyl chains. TMQA-C_8 was found to be a simple and low-cost organic semiconductor for the fabrication of OTFT device with potential practical application.

This work was supported by The Chinese Academy of Sciences–Croucher Foundation Funding Scheme for Joint Laboratories and HKU Seed Funding for Strategic Research Theme-Molecular Materials. We acknowledge Clover & Sunic Systems Ltd. for their support with the fabrication system housed at The University of Hong Kong (Grant No. HKU 200807176003).

[1] M. E. Roberts, S. C. B. Mannsfeld, R. M. Stoltenberg, and Z. N. Bao, Org. Electron. **10**, 377 (2009).
[2] M. Muccini, Nature Mater. **5**, 605 (2006).
[3] M. L. Chabinyc and A. Salleo, Chem. Mater. **16**, 4509 (2004).
[4] G. Horowitz, Adv. Mater. (Weinheim, Ger.) **10**, 365 (1998).
[5] H. Meng, F. P. Sun, M. B. Goldfinger, G. D. Jaycox, Z. G. Li, W. J. Marshall, and G. S. Blackman, J. Am. Chem. Soc. **127**, 2406 (2005).
[6] M. M. Payne, S. R. Parkin, J. E. Anthony, C. C. Kuo, and T. N. Jackson, J. Am. Chem. Soc. **127**, 4986 (2005).
[7] Y. J. Inoue, S. Z. Tokito, K. Ito, and T. Suzuki, J. Appl. Phys. **95**, 5795 (2004).
[8] C. D. Sheraw, T. N. Jackson, D. L. Eaton, and J. E. Anthony, Adv. Mater. (Weinheim, Ger.) **15**, 2009 (2003).
[9] J. Zhang, H. B. Wang, X. J. Yan, J. Wang, J. W. Shi, and D. H. Yan, Adv. Mater. (Weinheim, Ger.) **17**, 1191 (2005).
[10] K. Q. Ye, J. Wang, H. Sun, Y. Liu, Z. C. Mu, F. Li, S. M. Jiang, J. Y. Zhang, H. X. Zhang, Y. Wang, and C. M. Che, J. Phys. Chem. B **109**, 8008 (2005).
[11] E. M. Gross, J. D. Anderson, A. F. Slaterbeck, S. Thayumanavan, S. Barlow, Y. Zhang, S. R. Marder, H. K. Hall, M. Flore Nabor, J. F. Wang, E. A. Mash, N. R. Armstrong, and R. M. Wightman, J. Am. Chem. Soc. **122**, 4972 (2000).
[12] J. M. Shi and C. W. Tang, Appl. Phys. Lett. **70**, 1665 (1997).
[13] M. Hiramoto, S. Kawase, and M. Yokoyama, Jpn. J. Appl. Phys., Part 2 **35**, L349 (1996).
[14] See EPAPS supplementary material at http://dx.doi.org/10.1063/1.3233961 for the details of the synthesis, and TGA and transient curves.
[15] C. M. Che, H. F. Xiang, S. S. Y. Chui, Z. X. Xu, V. A. L. Roy, J. J. Yan, W. F. Fu, P. T. Lai, and I. D. Williams, Asian J. Chem. **3**, 1092 (2008).
[16] M. J. Wang, K. M. Liechti, Q. Wang, and J. M. White, Langmuir **21**, 1848 (2005).
[17] S. J. Kang, Y. Yi, C. Y. Kim, C. N. Whang, T. A. Callcott, K. Krochak, A. Moewes, and G. S. Chang, Appl. Phys. Lett. **86**, 232103 (2005).
[18] Y. L. Wu, Y. N. Li, S. Gardner, and B. S. Ong, J. Am. Chem. Soc. **127**, 614 (2005).